AMERICAN SOCIETY FOR MICROBIOLOGY | Molecular and Cellular Biology®

RESEARCH ARTICLE

USP49-Mediated Histone H2B Deubiquitination Regulates HCT116 Cell Proliferation through MDM2-p53 Axis

Lei Shi,[a] Xiangyu Shen,[b] Yuan Shen[b,c]

[a]School of Basic Medical Sciences, Xinxiang Medical University, Xinxiang, People's Republic of China
[b]School of Pharmacy, Xinxiang Medical University, Xinxiang, People's Republic of China
[c]Xinxiang Key Laboratory of Clinical Psychopharmacology, Xinxiang, People's Republic of China

ABSTRACT Posttranslational histone modifications play important roles in regulating chromatin structure and transcriptional regulation. Histone H2B monoubiquitination (H2Bub) is an essential regulator for transcriptional elongation and ongoing transcription. Here, we report that USP49, as a histone H2B deubiquitinase, is involved in HCT116 cell proliferation through modulating MDM2-p53 pathway genes. USP49 knockout contributes to increased HCT116 cell proliferation and migration. Importantly, USP49 knockout stimulated *MDM2* transcriptional levels and then inhibited the mRNA levels of *TP53* target genes. Conversely, the overexpression of USP49 suppressed *MDM2* gene expression and then promoted *TP53* target genes. Moreover, chromatin immunoprecipitation revealed that USP49 directly bound to the promoter of the *MDM2* gene. USP49 knockout increased H2Bub enrichment at the *MDM2* gene, whereas USP49 overexpression downregulated the H2Bub level at the *MDM2* gene. Therefore, our findings indicated that USP49-mediated H2B deubiquitination controls the transcription of MDM2-p53 axis genes in the process of HCT116 cell proliferation.

KEYWORDS USP49, deubiquitination, H2Bub, MDM2, p53, cell proliferation

Epigenetic posttranslational modifications, such as methylation, acetylation, and ubiquitylation of histone tails, crucially regulate gene transcription (1). Among these modifications, histone H2B monoubiquitination (H2Bub) has gained attention because it is highly associated with transcriptionally active loci and transcription elongation (2, 3). Cancer is frequently described as a disease of aberrant gene expression. Therefore, more and more connections between H2Bub and cancer have been discovered (4, 5). The loss of global H2Bub detected by immunohistochemical staining has been reported for a number of cancers, including breast (6), colorectal (7), lung (7), and parathyroid (8) cancers. Moreover, some H2Bub-modifying enzymes have been identified as oncogenes or tumor suppressors. RNF20, as the major H2B-specific E3 ubiquitin ligase in mammalian cells, may function as a tumor suppressor (9, 10). RNF20 depletion causes a global reduction of H2Bub levels and augments the expression of growth-promoting, prooncogenic genes (9, 10). RNF40, a binding partner of RNF20 and another major E3 for H2B monoubiquitination, also showed tumor-suppressive activity in breast cancer cells (11). Besides these, differential mutations have been reported in other H2Bub-associated E3 ubiquitin ligases in primary tumors, such as BRCA1 mutation in breast and ovarian cancers (12, 13). Therefore, a key mechanism of action of at least some of these changes in malignancy is probably through the dysregulation of H2Bub.

The TP53 gene, encoding the transcription factor p53, is mutated or deleted in half of human cancers, demonstrating the crucial role of p53 in tumor suppression (14). Importantly, p53 inactivation in cancers can also result from the amplification/overexpression of its specific inhibitor MDM2 (15, 16). Previous studies have shown that the stability and function of the p53 protein are controlled by MDM2 that targets p53 for

Address correspondence to Yuan Shen, s.y0001@163.com.

The authors declare no conflict of interest.

Received 7 September 2021
Returned for modification 28 September 2021
Accepted 10 January 2022
Accepted manuscript posted online 24 January 2022
Published 17 March 2022

degradation and directly inhibits p53 activity by binding to the transcriptional activation domain (17, 18). MDM2, as an important ubiquitin E3 ligase, combines with its binding partner MDMX to keep p53 activity after p53 transcriptional activities as well as to set up an efficient feedback loop to limit the p53 response (18, 19). p53 and its negative regulator MDM2 form the MDM2-p53 circuitry, which plays critical roles in regulating cancer cell growth, proliferation, cell cycle progression, apoptosis, senescence, angiogenesis, and the immune response (19). It is known that the stability of MDM2 is tightly controlled by the ubiquitin-proteasome system (20). A recent study showed that MARCH7, a RING domain-containing ubiquitin E3 ligase, catalyzes Lys63-linked polyubiquitination of MDM2, which impedes MDM2 autoubiquitination and degradation, thereby leading to the stabilization of MDM2 (21). Recently, the transcripts of *MDM2* have been reported to be regulated in tumorigenesis; however, the epigenetic regulation of *MDM2* remains not well understood.

Ubiquitin-specific proteases (USPs) are one protease family of deubiquitylating enzymes (DUBs). USPs contain a complex structure and a cysteine box (22). Some USPs have been reported to deubiquitinate H2Bub, including USP3 (23), USP7 (24), USP15 (25), USP22 (26), USP44 (27), and USP49 (28). Among these, USP7, one of the most studied deubiquitinating enzymes, contributes to cancer initiation and progression. USP7 is capable of deubiquitinating H2Bub (24) and has a broad range of other substrates, such as p53 (29), PTEN (30), FOXO4 (31), and PRC1/INK4a (32). USP7 also deubiquitinates MDM2, inhibiting MDM2 degradation and resulting in the polyubiquitination of p53, which leads to its degradation via the proteasome (33, 34). In this regard, USP7 acts as a cell cycle regulator through the protection of MDM2 and the degradation of p53, which promotes cell cycle progression and, consequently, cellular proliferation. USP49 has been identified as a novel H2Bub deubiquitinase (DUB) that regulates cotranscriptional pre-mRNA splicing (28). USP49 is also reported to suppress tumorigenesis and chemoresponses (35, 36). In pancreatic cancer, USP49 functions to deubiquitinate and stabilize FKBP51, which in turn enhances PHLPP's ability to dephosphorylate AKT (35). On the other hand, USP49 is capable of deubiquitinating and stabilizing the p53 protein in colorectal cancer (CRC) cells (36). USP49 knockdown renders cells more resistant to DNA damage and promotes tumorigenesis (36). Besides the effect on p53 protein stability, USP49 also has a positive effect on p53 transcriptional activity. The overexpression of USP49 stimulated p53 transcriptional activity and increased the mRNA levels of p53 target genes, whereas the knockdown of USP49 suppressed the expression of these genes (36). Here, we show that USP49 regulates MDM2-p53 pathway gene expression by modulating H2Bub levels in HCT116 cells. In our study, USP49 directly bound to the *MDM2* gene and deubiquitinated H2Bub at the locus of *MDM2*. The depletion of USP49 upregulated *MDM2* gene expression, resulting in decreased transcript levels of *TP53* and *TP53* target genes. Together, our results indicate that USP49 has an important role in regulating H2Bub and functions as an essential epigenetic enzyme in cell proliferation through mediating MDM2-p53 transcript levels.

RESULTS

USP49 knockout promotes colon cell proliferation. In order to investigate the biological role of USP49 in colon cells, the USP49-deficient HCT116 cell lines were created by CRISPR/Cas9 technology (37) (Fig. 1A). The USP49 knockout (USP49 KO) monoclones were identified by PCR amplification using sequencing primers (Fig. 1A and B). The sequencing results revealed that the frameshift mutation occurred in the target region of the USP49 gene (Fig. 1C). The USP49 knockout efficiency was confirmed by Western blotting. The expression levels of the USP49 protein were depleted in USP49-deficient HCT116 cells compared with the levels in the control HCT116 cells with the lentiCRISPRv2 empty vector (Fig. 1D). These results indicated that the USP49 gene was knocked out in HCT116 cells.

Next, we tested the effect of USP49 knockout on the growth of HCT116 cells. The proliferation rate was determined by a cell counting kit 8 (CCK8) assay. The knockout

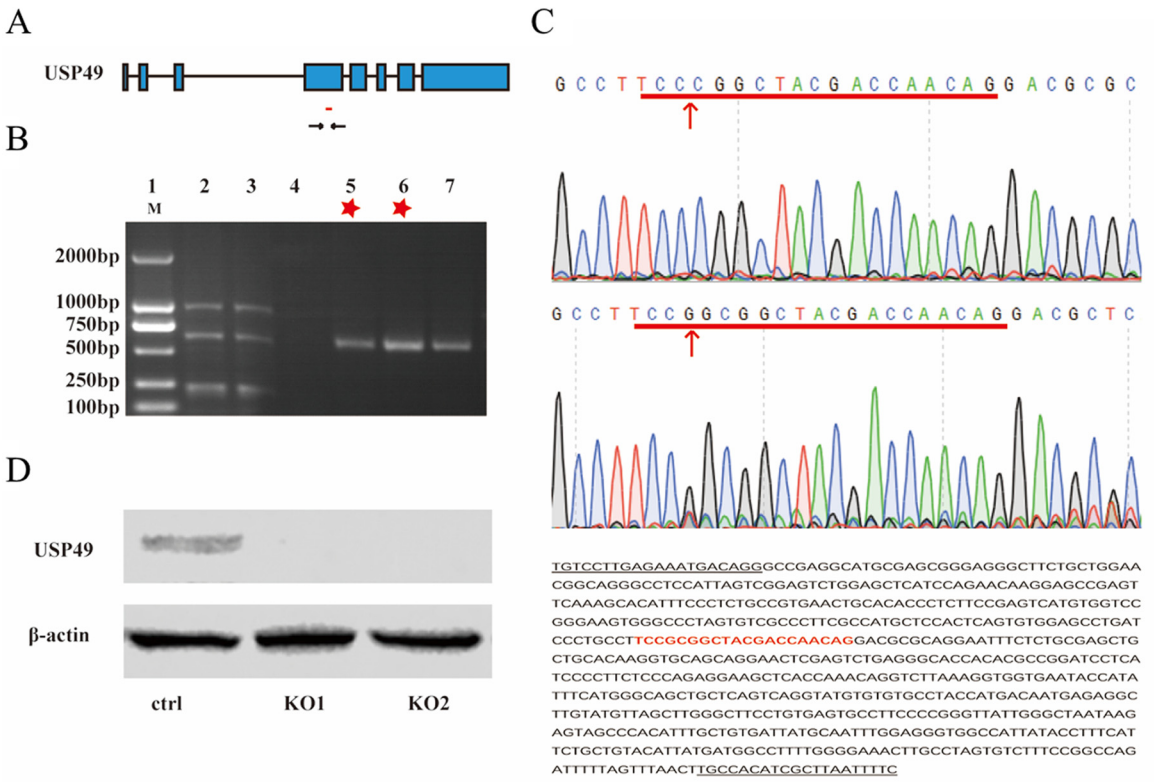

FIG 1 Identification of USP49 knockout using the CRISPR/Cas9 system in HCT116 cells. (A) Structure, designed sgRNA (red line), and PCR primers (black arrows) of the USP49 gene. (B) PCR amplification for USP49 sequences in the monoclones of USP49 knockout cell lines. The monoclones of lines 5 and 6 (red stars) were used for sequencing. M, molecular marker. (C) Sequencing analysis of USP49 knockout in monoclones 5 and 6. Sequencing results showed that the frameshift mutation occurred in the target region of the USP49 gene. There was one G deletion in monoclone 5 and one G addition in monoclone 6 (red arrows). PCR and sequencing primers are underlined in the following sequence. sgRNAs for USP49 are labeled in red in the sequence. (D) USP49 knockout monoclones were analyzed by Western blotting with antibodies against USP49 and actin.

of USP49 resulted in a significant increase in proliferation compared to control cells with an empty vector (Fig. 2A). To validate the enhanced proliferative effect of USP49 deficiency in HCT116 cells by an independent method, we performed colony formation assays. In accordance with the CCK8 results, colony formation assays showed that USP49 knockout in HCT116 cells leads to a strong increase of focus numbers. There were >100 colonies per well on average in USP49 knockout cells (out of 1,000 cells plated), while <20 colonies per well were observed in the vector control cells (Fig. 2B and C). These results suggested that USP49 plays important roles in regulating the tumorigenic abilities of colon cancer cells *in vitro*. In addition, scratch and transwell assays were conducted to evaluate the migration ability of USP49 knockout cells. The results revealed that the USP49-depleted cells possessed significantly increased migration capacities compared to the vector control cells (Fig. 2D to G). These findings indicate that USP49 acts as a suppressor of HCT116 cell proliferation and migration.

The effects of USP49 on HCT116 cells propelled us to explore its expression in primary CRC tissues. Consistent with our *in vitro* results, analysis of human patient tumor gene expression data generated by Gene Expression Profiling Interactive Analysis (GEPIA) (http://gepia.cancer-pku.cn/index.html) demonstrated that the USP49 expression level was significantly lower in colorectal adenocarcinoma than in the normal controls (Fig. 2H). A Kaplan-Meier survival analysis confirmed that cancer patients with low USP49 levels exhibited a significantly shorter survival time than patients with high USP49 levels ($P = 0.0181$ by a log rank test) (Fig. 2I), indicating that the level of USP49 was an informative prognostic factor for patients with colorectal adenocarcinoma. Taken together, these findings suggest that USP49 is downregulated in CRC and closely correlates with poor patient survival.

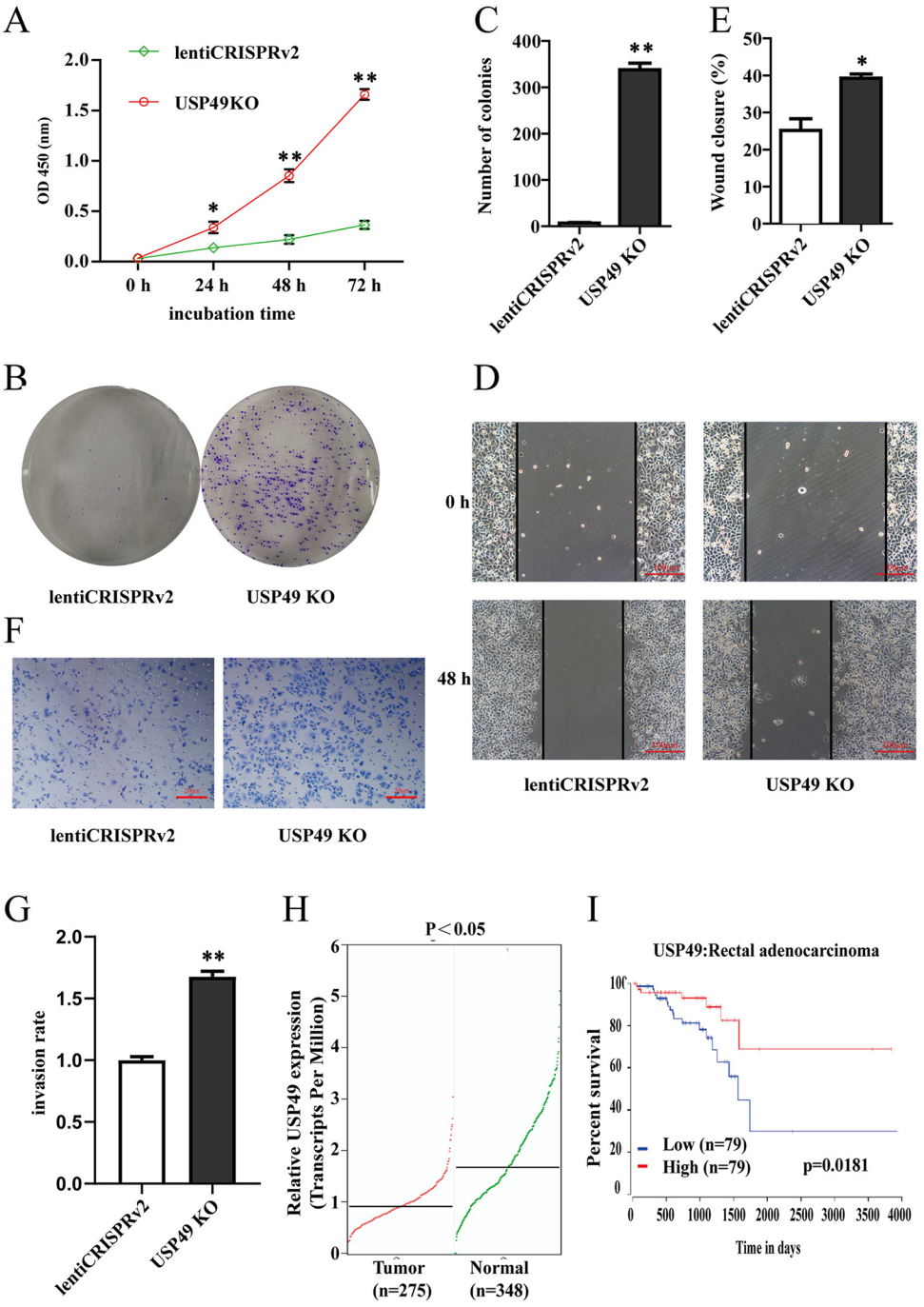

FIG 2 USP49 mediates cell proliferation of HCT116 cells. (A) USP49-depleted HCT116 cells displayed faster growth. Stable USP49 knockout (USP49 KO) cells and control cells transfected with an empty vector (lentiCRISPRv2) were seeded into 96-well plates, and the cell proliferation rates were monitored by a CCK8 assay. Quantitation was obtained from three biological replicates. *, $P < 0.05$; **, $P < 0.001$ (by Student's *t* test). OD, optical density. (B) Depletion of USP49 promoted cell proliferation. Cells were seeded in triplicate into 6-well plates and cultured for up to 12 days. The colonies were visualized by staining with crystal violet. (C) Quantitation of the colonies in the colony formation assay in panel B. Error bars represent SD from 3 biological experiments. **, $P < 0.001$ (by Student's *t* test). (D) A wound-healing migration assay reveals that the knockout of USP49 promotes cell migration. The wound migration assay was performed in stable USP49 KO and control (lentiCRISPRv2) cells. Representative images of wound sealing were collected on the day of the laceration and 2 days after the wound scratch. (E) The level of cell migration into the wound scratch was quantified as a percentage of wound healing. Quantitation was obtained from three independent measurements. *, $P < 0.05$ (by Student's *t* test). (F) Transwell assays were performed in USP49 KO and control (lentiCRISPRv2) cells. Representative images were captured 12 h after seeding 10^4 cells into the upper chamber. (G) Quantification of the results in panel F. Data are means ± SD from three independent experiments ($n = 3$). **, $P < 0.001$ (by

(Continued on next page)

The MDM2-p53 pathway is transcriptionally regulated by USP49. To confirm the effect of USP49 on cell growth, we transfected USP49 knockout cells with an expression vector encoding USP49 (pcDNA3-USP49). The CCK8, colony formation, and transwell experiments revealed that knockout cells transfected with a USP49-expressing vector partially abolished the phenotypes of enhanced proliferative and migration activities induced in USP49 knockout cells (Fig. 3A to E). To investigate the underlying mechanism of USP49 knockout-promoted proliferation, we tested the effect of USP49 knockout on cell cycle-related molecules. As shown in Fig. 3F, real-time quantitative PCR (RT-qPCR) analysis revealed that the transcript level of *MDM2* was significantly increased, whereas the mRNA expression level of the *TP53* gene was decreased, in the USP49 knockout cells. In addition, the depletion of USP49 resulted in significant reductions of the *TP53* downstream genes, such as *CDKN1A*/*p21* and *BAX*. Furthermore, the transfection of pcDNA3-USP49 into the knockout cells resulted in a reduction of the *MDM2* mRNA level as well as increases in *TP53*, *CDKN1A*, and *BAX* transcripts, which were partially reversed by the USP49 knockout-induced effect (Fig. 3F). The downregulated transcript expression levels of *TP53* and its target genes *CDKN1A* and *BAX* in USP49 knockout cells were consistent with the change in gene expression in USP49 knockdown HCT116 cells from a previous report (36). We also determined whether the loss of USP49 affects MDM2 and p53 protein levels. The results showed that the knockout of USP49 significantly increased the MDM2 protein level and suppressed the p53 protein level, whereas the transfection of pcDNA3-USP49 into knockout cells partially rescued this effect (Fig. 3G). To confirm the effect of USP49 on the transcriptional regulation of MDM2-p53 pathway genes, we transfected HCT116 cells with pcDNA3-Flag and an empty vector (pcDNA3), respectively. The expression levels of USP49 mRNA and protein were significantly increased in the USP49-overexpressing (OE) HCT116 cells compared with the control HCT116 cells with pCDNA3 (Fig. 3H and I). RT-qPCR showed that the mRNA level of *MDM2* was decreased, whereas those of *TP53*, *CDKN1A*, and *BAX* were increased, in USP49-overexpressing cells (Fig. 3J). Together, these results suggested that USP49 affects HCT116 cell growth by regulating the transcripts of the MDM2-p53 axis.

USP49-mediated H2B deubiquitination in HCT116 cells. A previous study showed that USP49 deubiquitinates histone H2Bub and regulates cotranscriptional pre-mRNA splicing (28). To determine whether USP49 mediates H2B deubiquitination in cancer malignancy, we first extracted the total histones and detected the global H2Bub level in USP49 knockout HCT116 cells. As shown in Fig. 4A, the levels of H2Bub were strongly increased in USP49 knockout HCT116 cells. To further determine the function of USP49 in H2Bub deubiquitination in HCT116 cells, the knockout cells were transfected with gradient concentrations of the pcDNA3-USP49 plasmid. The hypotonic lysis solutions of these cells in the process of extracting histone were examined for USP49 levels. As shown in Fig. 4C (top), the transfection of pcDNA3-USP49 generated a dose-dependent increase in the USP49 protein level. Next, we examined the H2Bub levels in these cells and found that the H2Bub levels were gradually decreased with increasing USP49 levels (Fig. 4C). These results suggested that USP49 acted as a deubiquitinase for H2Bub in the process of cell proliferation.

USP49 regulated MDM2 transcription via modifying H2Bub. H2Bub, a well-known epigenetic modification mark, is linked to transcriptionally active loci and transcription

FIG 2 Legend (Continued)
Student's *t* test). (H) The expression level of USP49 in CRC tissues was analyzed by Gene Expression Profiling Interactive Analysis (GEPIA), matched with data from The Cancer Genome Atlas (TCGA) public cancer database and the Genotype-Tissue Expression (GTEx) database (http://gepia.cancer-pku.cn). Lower expression levels of USP49 were detected in 275 CRC tissue samples than in 348 normal tissue samples. Each dot represents the expression of a CRC sample and the paired normal tissue sample, and black lines indicate the median values. (I) Effects of the USP49 expression level on CRC patient survival. Kaplan-Meier survival curves revealed an association of low USP49 levels with shorter overall survival in CRC patients. The data on USP49 mRNA expression in 158 CRC patients were downloaded from the oncoLnc database (http://www.oncolnc.org). USP49 expression levels above the median value were defined as the high-expression group, whereas USP49 expression levels below the median value were defined as the low-expression group.

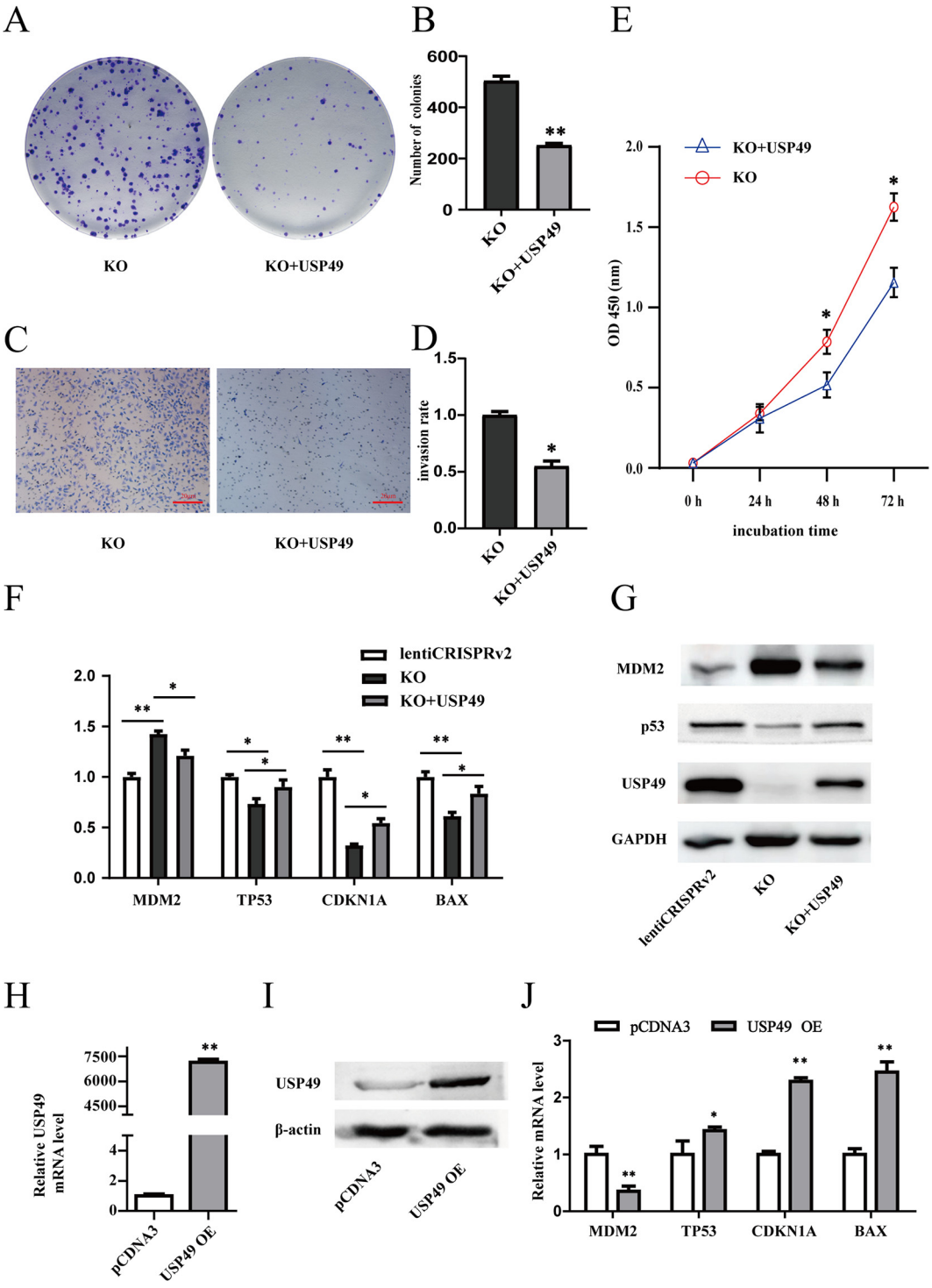

FIG 3 USP49 regulates the expression of MDM2-p53 pathway genes. (A and B) Transfection of pcDNA3-USP49 into knockout (KO) cells leads to slower growth than in KO cells. A colony formation assay was performed in KO cells and knockout cells transfected with the USP49 expression vector (KO+USP49) after 12 days of culture. The data are presented as means ± SD (n = 3). *, $P < 0.05$ (by Student's t test). (C and D) A transwell migration assay was performed in KO and KO+USP49 cells. Data are means ± SD from three independent experiments (n = 3). *, $P < 0.05$. (E) Cell proliferation was assessed by a CCK8 assay at the indicated times. Quantitation was obtained from three biological replicates. The data are shown as means ± SD (n = 3). *, $P < 0.05$ (by Student's t test). (F) RT-qPCR analysis of the transcript levels of the *MDM2*, *TP53*, *CDKN1A*, and *BAX* genes in stable USP49 KO cells, KO+USP49 cells, and control cells with the empty vector (lentiCRISPRv2). Bars are means ± SD of data from three biological replicates. *, $P < 0.05$; **, $P < 0.001$ (by Student's t test). (G) Immunoblot analysis was performed using anti-USP49, anti-MDM2, and anti-p53 specific antibodies in control (lentiCRISPRv2), USP49 KO, and KO+USP49 cells. (H and I) mRNA and protein levels of USP49 in USP49-overexpressing

(Continued on next page)

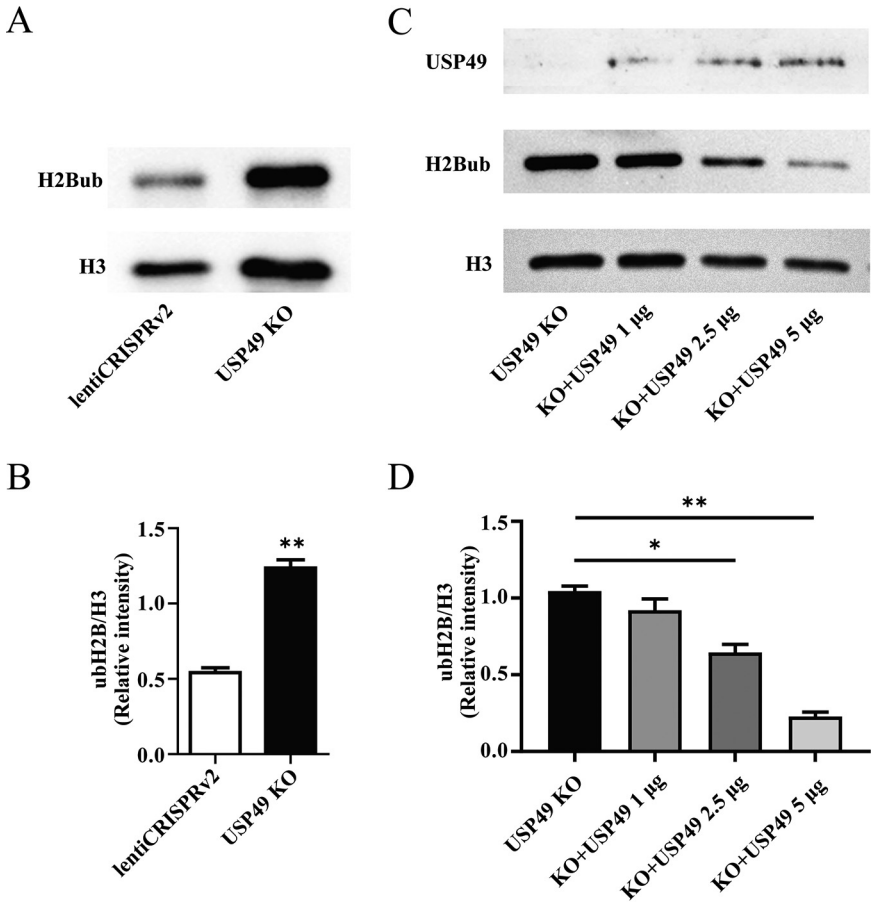

FIG 4 USP49 mediated H2Bub levels in HCT116 cells. (A) Immunoblotting showed that the knockout of USP49 increased the level of H2Bub in HCT116 cells. Histones were extracted from stable USP49 knockout cells and control cells. Antibodies against H2Bub and H3 were used. (B) Quantification of the results in panel A. The band intensities were measured and analyzed using ImageJ software, and the levels of H2Bub were normalized to that of H3, which was used as a loading control. Bars are means ± SD from 3 biological replicates. Significant differences were tested by Student's *t* test (**, $P < 0.001$). (C) Transfection of pcDNA3-USP49 into knockout cells generated a dose-dependent decrease in the H2Bub level. Immunoblotting of knockout cells transfected with the USP49 expression vector (pcDNA3-USP49), as indicated at the bottom, was performed. The cells were harvested, and histones were extracted 48 h later. The hypotonic lysis solutions from these cells during the histone extraction procedures were used for the detection of USP49 amounts (top). (D) Quantification of the results in panel C. Bars are means ± SD from 3 biological replicates. ** indicates a *P* value of <0.001.

elongation (3). Since H2Bub has high enrichment in MDM2-p53 pathway genes (including *MDM2*) in cancer cells following DNA damage and H2Bub enrichment was normally associated with the increased expression of these genes (38), we postulated that USP49 may modulate the gene expression of *MDM2* by mediating the H2Bub level in cell proliferation. To validate this hypothesis, we first tested the H2Bub levels on the MDM2-p53 pathway genes. By using a chromatin immunoprecipitation (ChIP)-qPCR assay, we found that H2Bub enrichment at the promoter and gene body of *MDM2* was higher in USP49-deficient cells than in the control cells with an empty vector (promoter, 1.99 ± 0.09 in KO versus 1.12 ± 0.10 in control cells; gene body, 2.17 ± 0.12 in KO versus 1.69 ± 0.11 in control cells), whereas the H2Bub levels at the *BAX* and *CDKN1A* genes were decreased

FIG 3 Legend (Continued)
(USP49 OE) cells. Cells transfected with the USP49 expression vector (pcDNA3-USP49) (USP49 OE) and an empty vector (pcDNA3) (control) were harvested, and expression levels were measured 48 h later. (J) RT-qPCR analysis of the mRNA levels of the *MDM2*, *TP53*, *CDKN1A*, and *BAX* genes in USP49-overexpressing cell lines compared to the control cell lines with the empty vector (pcDNA3). Bars are means ± SD of data from three biological replicates. *, $P < 0.05$; **, $P < 0.001$ (by Student's *t* test).

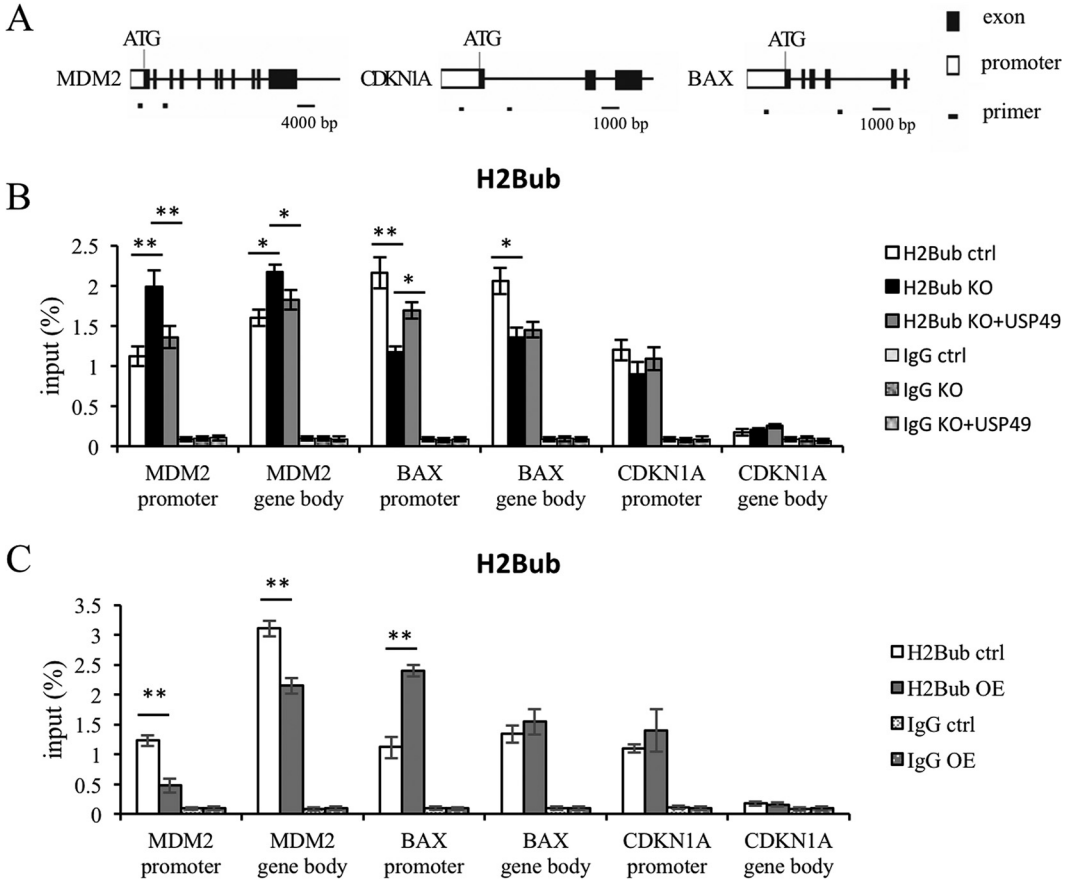

FIG 5 USP49 modulated H2Bub levels on the MDM2-p53 pathway genes. (A) Structures and ChIP-tested promoter and gene body regions of the *MDM2*, *CDKN1A*, and *BAX* genes that were dysregulated in USP49 knockout or overexpression cells (Fig. 3). (B) ChIP analysis of H2Bub levels of the *MDM2*, *CDKN1A*, and *BAX* genes in stable USP49 knockout cells compared with the empty vector cells. Results are presented as a percentage of the input. Bars are means ± SD of data from three biological replicates (*, $P < 0.05$; **, $P < 0.001$ [by Student's *t* test]). (C) ChIP analysis of H2Bub levels of the *MDM2*, *CDKN1A*, and *BAX* genes in cells transfected with the USP49 expression vector (USP49 OE) or pcDNA3 (control).

or showed no change in USP49 KO cells compared with the cells containing the empty vector (Fig. 5A and B). The transfection of pcDNA3-USP49 into knockout cells resulted in relative declines of H2Bub levels at the MDM2 loci (promoter, 1.36 ± 0.07 in KO+USP49 versus 1.99 ± 0.09 in KO cells; gene body, 1.83 ± 0.11 in KO+USP49 versus 2.17 ± 0.12 in KO cells) (Fig. 5B). To confirm that USP49 modulates the H2Bub levels at the MDM2-p53 pathway genes, we also transfected HCT116 cells with pcDNA3-USP49 and the empty vector pcDNA3, respectively. ChIP-qPCR showed that H2Bub levels were lower at the *MDM2* loci in USP49-overexpressing cells than in the empty vector cells (promoter, 0.95 ± 0.08 in OE versus 1.23 ± 0.11 in control cells; gene body, 2.15 ± 0.12 in OE versus 3.10 ± 0.21 in control cells), whereas they were higher at *BAX* and showed almost no change at the *CDKN1A* gene (Fig. 5C). Therefore, USP49 may transcriptionally regulate MDM2-p53 pathway genes via modulating H2Bub levels.

USP49 bound directly to the *MDM2* gene for deubiquitinating H2Bub. Since USP49 specifically repressed the expression and deubiquitinated H2Bub levels of the *MDM2* gene, we then investigated whether USP49 could directly target the *MDM2* gene for epigenetic regulation. We used transfected USP49-overexpressing HCT116 cells and specific anti-USP49 antibody. Chromatin immunoprecipitation revealed an increase in the binding signal of USP49 for the promoter and gene body of *MDM2* in the USP49-overexpressing cells compared to that in the control cells with the empty vector (promoter, 0.122 ± 0.009 in OE versus 0.081 ± 0.007 in control cells; gene body,

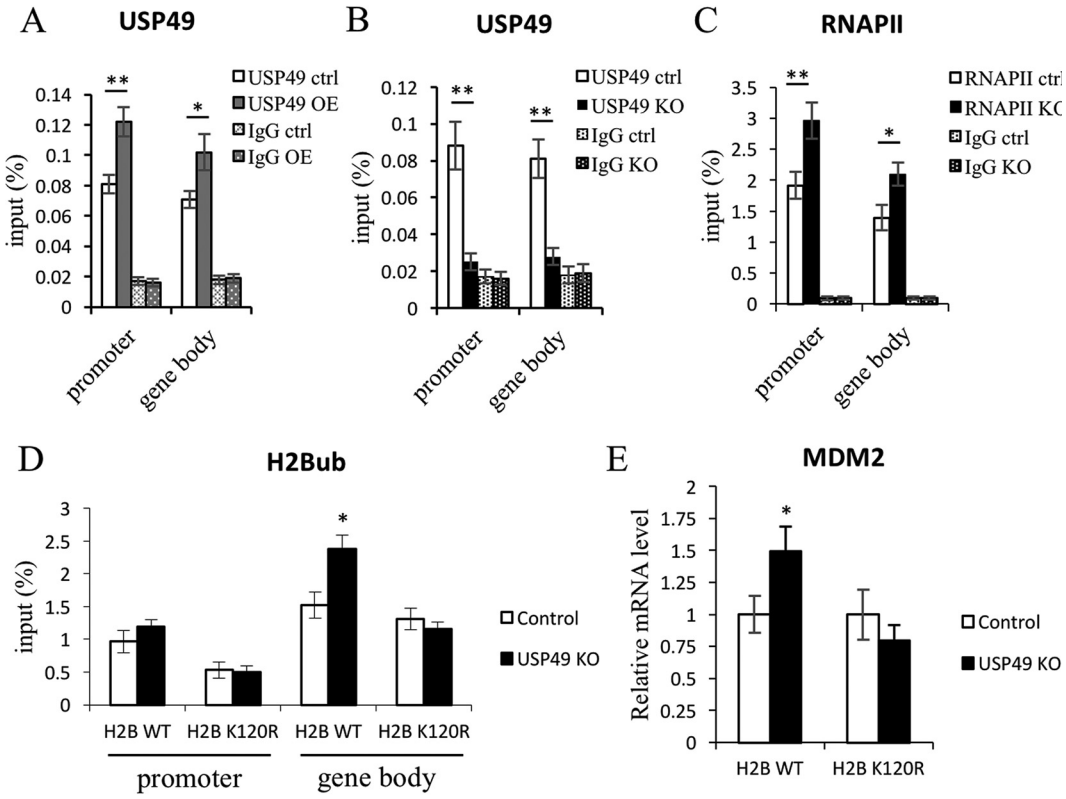

FIG 6 USP49 regulates MDM2 mRNA expression through deubiquitinating H2Bub. (A) ChIP analysis of USP49 binding to the *MDM2* gene. The abundances of MDM2 fragments immunoprecipitated by USP49-specific antibody in cells transfected with the USP49 expression vector (USP49 OE) or pcDNA3 (control) were determined. *, $P < 0.05$; **, $P < 0.001$ (by Student's *t* test). (B) ChIP analysis of USP49 levels at the *MDM2* gene in stable USP49 knockout cells compared with empty vector cells. *, $P < 0.05$; **, $P < 0.001$ (by Student's *t* test). (C) ChIP analysis of RNAPII enrichment at the *MDM2* gene in stable USP49 knockout (USP49 KO) cells compared with the control cells (empty vector [lentiCRISPRv2]). *, $P < 0.05$; **, $P < 0.001$ (by Student's *t* test). (D) ChIP analysis of H2Bub levels at the *MDM2* loci in control and USP49 KO cells transfected with H2B and the H2B K120R mutant. Transfection of wild-type (WT) H2B increased the H2Bub level at the gene body of MDM2 in USP49 KO cells. (E) mRNA levels of the *MDM2* gene in control and USP49 KO cells transfected with wild-type H2B and the H2B K120R mutant. Transfection of wild-type H2B does not interfere with the USP49 knockout-induced increase of MDM2 transcripts, but transfection of H2B K120R suppresses the effect.

0.102 ± 0.011 in OE versus 0.071 ± 0.006 in control cells) (Fig. 6A). To confirm the binding of USP49 to the *MDM2* promoter, we also tested the binding signal of USP49 in knockout cells. The results showed that there was no obvious enrichment of the USP49 binding signal to the *MDM2* gene in USP49 knockout cells (Fig. 6B). Therefore, USP49 directly targets the *MDM2* gene and functions as a deubiquitinase to regulate H2Bub at the *MDM2* loci. It has been shown that H2Bub facilitates RNA polymerase II (RNAPII)-dependent transcription (2). To determine whether the loss of USP49 affects RNAPII enrichment at MDM2, we performed a ChIP experiment with anti-RNAPII antibody. As shown in Fig. 6C, the knockout of USP49 increased RNAPII enrichment at the promoter and gene body region of MDM2 (Fig. 6C), suggesting that USP49 may regulate MDM2 transcription via H2Bub and RNAPII enrichment. To ensure that the increasing H2Bub levels at the *MDM2* loci in USP49 knockout cells affected gene expression, we transfected wild-type H2B and the ubiquitination site mutant H2B K120R into control (lentiCRISPRv2) and USP49 knockout (USP49 KO) cells and measured the effects on H2Bub and the gene expression of MDM2. As shown in Fig. 6D and E, the transfection of wild-type histone H2B kept the elevation of H2Bub and the gene expression of MDM2 induced by USP49 knockout; however, the transfection of the H2B mutant affected USP49 knockout-induced H2Bub and gene expression (Fig. 6D and E). Therefore, these results demonstrate that USP49 regulates *MDM2* expression through H2Bub deubiquitination.

DISCUSSION

The human genome encodes approximately 100 putative deubiquitinases (DUBs), which are divided into seven DUB subfamilies based on structure, including the ubiquitin-specific protease (USP) subfamily, the ubiquitin C-terminal hydrolase (UCH) subfamily, the Machado-Joseph disease protein domain protease (MJD) subfamily, the ovarian tumor protease (OTUs) subfamily, the JAMM (JAB1/MPN/Mov34 metalloenzyme) motif protease subfamily, the motif interacting with ubiquitin-containing novel DUB (MINDY) subfamily, and the zinc finger with UFM1-specific peptidase (ZUFSP) subfamily (22, 39). Dysregulated deubiquitinase expression is frequently associated with tumorigenesis and poor prognoses in clinical patients with CRC. The expression levels of USP1 (40), USP4 (41, 42), USP5 (43), USP20 (44), USP28 (45), USP47 (46), and UCHL1 (47) were found to be significantly elevated in CRC, and the increased expression levels were correlated with shorter overall survival and advanced stages of cancers. On the other hand, USP22, USP46, and USP49 may function as tumor suppressors in CRC with different mechanisms (48–50). USP22 suppressed CRC tumorigenesis by decreasing mTOR activity (48). USP46 exerted tumor-suppressive function by controlling the PHLPP-dependent attenuation of Akt signaling (49). USP49 may act as a tumor suppressor by interacting with p53 and suppressing its ubiquitination (36). Here, we showed that USP49 epigenetically regulated *MDM2* gene expression in HCT116 cell proliferation. Therefore, USP49 functions as a tumor suppressor in CRC by modulating the MDM2-p53 axis through multiple mechanisms.

H2Bub is a central histone modification associated with an open chromatin configuration and the promotion of transcriptional elongation. Regions of H2Bub enrichment regulate the accessibility of genomic sites. Previous studies have shown that H2Bub is enriched downstream of the transcription start sites of a group of specific genes that are the most highly enriched in the p53 signaling pathway, including *MDM2* and *CDKN1A* (38). Here, we showed that the depletion of USP49 leads to an obvious increase of the H2Bub level at the *MDM2* gene loci, whereas there was a decrease or no change of the H2Bub level at the *BAX* and *CDKN1A* loci. These results indicate that USP49 depletion resulted in higher enrichment of H2Bub at the *MDM2* loci, allowing increased *MDM2* expression via transcriptional elongation and thus facilitating its function, which is also consistent with previous results showing enhanced H2Bub levels and increased expression levels of the *MDM2* gene in cancer cells (38). Many tumors exhibit amplification of the *MDM2* gene or high MDM2 protein levels. Recently, the *MDM2* transcript level has been reported to be regulated in tumorigenesis. For example, microRNA 1827 (miR-1827) and miR-339-5p negatively regulated *MDM2* mRNA, which in turn affected p53 protein levels and p53-governed cellular responses such as proliferation arrest (50, 51). Inhibition of HDAC2 reduces *MDM2* mRNA expression and reduces tumor growth (52). The results presented here suggest that USP49 epigenetically regulates *MDM2* mRNA expression through modulating the H2Bub level and in turn impacts *TP53* and *TP53* downstream genes in tumorigenesis. Of note, the *TP53* gene itself was not enriched by H2Bub in HCT116 cells in the current study (data not shown), which was consistent with ChIP sequencing (ChIP-seq) results showing no obvious H2Bub enrichment at the *TP53* gene in cancer cells after DNA damage (38). Indeed, it has been long established that the stabilization of p53 leading to increased levels of this tumor suppressor protein is due to posttranslational modifications, including acetylation and ubiquitination, rather than being predominantly a transcriptional event (29, 53). It is interesting that p53 protein stability is controlled by USP49 via interacting with p53 and suppressing its ubiquitination in the nucleus (36). Taken together, USP49 regulates the MDM2-p53 pathway at both the transcriptional and posttranslational levels.

MATERIALS AND METHODS

Cell culture. HEK293T and human colorectal carcinoma HCT116 cell lines were cultured in Dulbecco's modified Eagle's medium (DMEM) (HyClone) supplemented with 10% fetal bovine serum (FBS) (HyClone) at 37°C in a 5% CO_2 incubator. USP49 gene knockout HCT116 cell lines were generated

as described below. The pCDNA3-USP49-Flag expression vector, wild-type H2B, and the ubiquitination site mutant H2B K120R vector were obtained from Hengbin Wang (28).

Establishment of USP49 knockout cell lines. USP49 knockout cell lines were established by using a lentivirus-based CRISPR/Cas9 system (37). The single guide RNA (sgRNA) sequences chosen for USP49 were 5′-CACCGCTGTTGGTCGTAGCCGCGGA-3′ (forward) and 5′-AAACTCCGCGGCTACGACCAACAGC-3′ (reverse). Annealed double-stranded sgRNA oligonucleotides were ligated into the lentiCRISPRv2 vector (Addgene plasmid 52961), which coexpressed Cas9 and sgRNA in the same vector. The constructed lentivirus-based CRISPR vectors were prepared and packaged according to an established protocol (37). Subsequently, HCT116 cells were infected with sgRNA-encoding lentivirus and cultured in DMEM supplemented with 10% FBS. The infected cells were then cultured in DMEM containing 3 μg/mL puromycin for 14 days of selection. Surviving cells were plated onto 96-well plates with 1 cell per well. Colonies that emerged from single cells were selected and expanded for sequencing analysis. The primers used to amplify USP49 gene sequences surrounding the target gene site were 5′-TGTCCTTGAGAAATG ACAGG-3′ (forward) and 5′-GAAAATTAAGCGATGTGGCA-3′ (reverse). PCR products were purified and then subjected to Sanger sequencing to verify gene disruption.

Growth curve. The cell proliferation rates were measured by using cell counting kit 8 (Dojindo Molecular Technologies, Japan) to generate cell growth curves. In brief, cells were seeded into 96-well plates at a density of 2,000 cells/well in 100 μL culture medium. Cell proliferation was determined at 0, 24, 48, and 72 h according to the manufacturer's protocol. The absorbance at 450 nm was measured using a microplate reader (Bio-Tek, USA). Quantitation was obtained from three biological replicates.

Colony formation. Cells were seeded into 6-well plates with 1,000 cells per well and cultured in medium containing 10% FBS for 12 days, replacing the medium with new medium every 3 days. Colonies were fixed with 4% formaldehyde for 20 min and stained with a crystal violet solution (catalog number E607309; Sangon Biotech) for 20 min. The number of colonies with more than 50 cells was counted. For each group, wells were counted in triplicate.

Scratch assay. Cells were seeded into 6-well plates at 3.5×10^5 cells per well and incubated at 37°C for 12 h to adhere and spread completely. A P1000 pipette tip was used to create a straight line in the cell monolayer. The plates were washed three times with phosphate-buffered saline (PBS) and replaced with medium containing 2% serum. After incubation at 37°C for 48 h, the plates were washed with PBS and photographed. For each image, distances between one side of the scratch and the other were measured.

Transwell assay. A total of 1×10^4 cells were added to the upper 8-μm pore inserts (Millipore) in serum-free medium. The lower chamber was filled with 20% FBS medium as a chemoattractant. After the indicated time of culture at 37°C in an incubator with 5% CO_2, cells that migrated through the inserts were fixed with methanol and stained with crystal violet.

Western blotting. Cells were washed with PBS and then lysed in radioimmunoprecipitation assay (RIPA) buffer supplemented with protease inhibitors. Equal amounts of proteins were separated by SDS-PAGE and transferred to a polyvinylidene difluoride (PVDF) membrane. Membranes were incubated overnight at 4°C using specific antibodies for USP49 (catalog number 18066-1-AP; Proteintech), H2Bub (catalog number 5546; Cell Signaling Technology), histone H3 (catalog number ab1791; Abcam), MDM2 (catalog number 27883-1-AP; Proteintech), p53 (catalog number 10442-1-AP; Proteintech), glyceraldehyde-3-phosphate dehydrogenase (GAPDH) (catalog number 10494-1-AP; Proteintech), and beta-actin (catalog number 4970; Cell Signaling Technology), followed by secondary antibodies conjugated to horseradish peroxidase (HRP). Proteins were visualized using enhanced chemiluminescence (ECL) detection agents (Immobilon; Millipore).

Histone extraction. Histone extraction was performed essentially as described previously (54). In brief, cells were harvested and washed twice with ice-cold PBS. Then cell pellet was resuspended in hypotonic lysis buffer (10 mM Tris-Cl [pH 8.0], 1 mM KCl, 1.5 mM $MgCl_2$, 1 mM dithiothreitol [DTT], and protease inhibitors) to promote hypotonic swelling of cells. Cell nuclei were harvested by centrifugation and resuspended in a 0.4 M H_2SO_4 solution. The histones were extracted with acid overnight at 4°C. After centrifugation, the supernatant

TABLE 1 Primers used for RT-qPCR

Primer name	Sequence (5′–3′)
β-actin-RT-F	TGGCACCACCTTCTACAATGA
β-actin-RT-R	CAGCCTGGATAGCAACGTACAT
USP49-RT-F	GAGCCCTTTTGGGACCTATC
USP49-RT-R	AGGGCCTCTGTCTCTGTGAA
P53-RT-F	CTTCCCTGGATTGGCCA
P53-RT-R	TCTGAAAATGTTTCCTGACTCAGA
P21-RT-F	GATGGAACTTCGACTTTGTCAC
P21-RT-R	GTCCACATGGTCTTCCTCTG
BAX-RT-F	CGAACTGGACAGTAACATGGAG
BAX-RT-R	CAGTTTGCTGGCAAAGTAGAAA
MDM2-RT-F	CTTCTAGGAGATTTGTTTGGCG
MDM2-RT-R	ATGTACCTGAGTCCGATGATTC
GAPDH-RT-F	CCAGCAAGAGCACAAGAGGAAGAG
GAPDH-RT-R	GGTCTACATGGCAACTGTGAGGAG

TABLE 2 Primers used for ChIP-qPCR

Primer name	Sequence (5′–3′)
MDM2(coding)-F	CAGGCTCCTTGCATACAGGT
MDM2(coding)-R	CCCAGGTCCCTCAACTACAA
MDM2(UTR)-F	CTTGAGGCCAGGAGTTTGAG
MDM2(UTR)-R	AGAGTGTAGTGGCGCAATCA
GAPDH(ChIP)-F	CCGGGAGAAGCTGAGTCATG
GAPDH(ChIP)-R	TTTGCGGTGGAAATGTCCTT
P53(coding)-F	CGCCAACTCTCTCTAGCTCG
P53(coding)-R	AGGGCAGGGGAGTACTGTAG
P53(UTR)-F	GCAGCCAGTCTAGCTAGAGC
P53(UTR)-R	GCTCACCTGCCCATTCTCTT
P21(coding)-F	GACTTGCGAGCGGTTTTGTT
P21(coding)-R	TCTTGTGCCGTCTCTGACAC
P21(UTR)-F	ATCTGACGAGCCCTCAGTCT
P21(UTR)-R	TTTGCAGCAGACACAATGGC
BAX(coding)-F	CCTGGGGATCGTGGTATCAA
BAX(coding)-R	AGGGATGTAGCCTGCTTTGT
BAX(UTR)-F	TTCTCTTTGTGGGCCTGAAG
BAX(UTR)-R	TTTTCTGGGAGTGGAAATGG

solution containing histones was transferred into a fresh tube. The histones were precipitated with additional trichloroacetic acid (TCA) drop by drop (the final concentration of TCA was 33%). TCA precipitates were recovered by centrifugation at 16,000 $\times$ *g* for 10 min at 4°C and washed twice with ice-cold acetone. The histone pellets were air dried and stored at −20°C until use.

Quantitative real-time PCR. Total RNA was extracted from cells using TRIzol (catalog number 9108Q; TaKaRa). Reverse transcription of 1 μg of RNA was done using the Prime reagent kit with gDNA Eraser (catalog number RR047A; TaKaRa) according to the manufacturer's instructions. Quantitative real-time PCR was done using SYBR green PCR master mix (catalog number RR820A; TaKaRa) in a total volume of 20 μL on the LightCycler 480II system (Roche, USA), as follows: 95°C for 30 s followed by 40 cycles of 95°C for 5 s, 60°C for 30 s, and 72°C for 30 s. The sequences of the primer pairs used for qPCR are shown in Table 1. β-Actin was used as the reference gene. The relative levels of gene expression were calculated by the $2^{-\Delta\Delta CT}$ method. Experiments were repeated in triplicate.

Chromatin immunoprecipitation. ChIP was performed essentially as described previously (48). Briefly, cells were cross-linked with 1% formaldehyde for 10 min at room temperature and quenched with 125 mM glycine for 5 min. Soluble chromatin was obtained after cell lysis and sonication. The samples were then precleared and incubated with 3 to 5 μg antibody-loaded Dynabeads protein A (catalog number 10002D; Invitrogen) at 4°C overnight. Subsequently, the immunoprecipitated DNA was de-cross-linked, purified, and analyzed by qPCR. ChIP-qPCR was done with anti-USP49 antibody (catalog number 18066-1-AP; Proteintech), anti-RNAPII antibody (catalog number ab5408; Abcam), or anti-H2Bub antibody (catalog number 5546; Cell Signaling Technology). Primers used for ChIP-qPCR are listed in Table 2.

Statistical analysis. Data determined as means $\pm$ standard deviations (SD) were analyzed via SPSS software. Experiments were conducted three times. One-way/two-way analysis of variance (ANOVA) or Student's *t* test was used for difference analysis (*, $P < 0.05$; **, $P < 0.001$).

Availability of data. All of the data and material in this paper are available upon request.

ACKNOWLEDGMENTS

We are grateful to members of Hengbin Wang's lab for critical discussion and excellent technical assistance.

This work was supported by the National Natural Science Foundation of China (number 31500982) and doctoral starting funds from Xinxiang Medical University (number 505197).

We declare no conflicts of interest.

REFERENCES

1. Allis CD, Jenuwein T, Caparros M, Reinberg D (ed). 2007. Epigenetics. Cold Spring Harbor Laboratory Press, Cold Spring Harbor, NY.
2. Pavri R, Zhu B, Li G, Trojer P, Mandal S, Shilatifard A, Reinberg D. 2006. Histone H2B monoubiquitination functions cooperatively with FACT to regulate elongation by RNA polymerase II. Cell 125:703–717. https://doi.org/10.1016/j.cell.2006.04.029.
3. Minsky N, Shema E, Field Y, Schuster M, Segal E, Oren M. 2008. Monoubiquitinated H2B is associated with the transcribed region of highly expressed genes in human cells. Nat Cell Biol 10:483–488. https://doi.org/10.1038/ncb1712.
4. Espinosa JM. 2008. Histone H2B ubiquitination: the cancer connection. Genes Dev 22:2743–2749. https://doi.org/10.1101/gad.1732108.
5. Cole AJ, Clifton-Bligh R, Marsh DJ. 2015. Histone H2B monoubiquitination: roles to play in human malignancy. Endocr Relat Cancer 22:T19–T33. https://doi.org/10.1530/ERC-14-0185.
6. Prenzel T, Begus-Nahrmann Y, Kramer F, Hennion M, Hsu C, Gorsler T, Hintermair C, Eick D, Kremmer E, Simons M, Beissbarth T, Johnsen SA. 2011. Estrogen-dependent gene transcription in human breast cancer cells relies upon proteasome-dependent monoubiquitination of histone H2B. Cancer Res 71:5739–5753. https://doi.org/10.1158/0008-5472.CAN-11-1896.

7. Urasaki Y, Heath L, Xu CW. 2012. Coupling of glucose deprivation with impaired histone H2B monoubiquitination in tumors. PLoS One 7:e36775. https://doi.org/10.1371/journal.pone.0036775.
8. Hahn MA, Dickson KA, Jackson S, Clarkson A, Gill AJ, Marsh DJ. 2012. The tumor suppressor CDC73 interacts with the ring finger proteins RNF20 and RNF40 and is required for the maintenance of histone 2B monoubiquitination. Hum Mol Genet 21:559–568. https://doi.org/10.1093/hmg/ddr490.
9. Shema E, Tirosh I, Aylon Y, Huang J, Ye C, Moskovits N, Raver-Shapira N, Minsky N, Pirngruber J, Tarcic G, Hublarova P, Moyal L, Gana-Weisz M, Shiloh Y, Yarden Y, Johnsen SA, Vojtesek B, Berger SL, Oren M. 2008. The histone H2B-specific ubiquitin ligase RNF20/hBRE1 acts as a putative tumor suppressor through selective regulation of gene expression. Genes Dev 22:2664–2676. https://doi.org/10.1101/gad.1703008.
10. Shema E, Kim J, Roeder RG, Oren M. 2011. RNF20 inhibits TFIIS-facilitated transcriptional elongation to suppress pro-oncogenic gene expression. Mol Cell 42:477–488. https://doi.org/10.1016/j.molcel.2011.03.011.
11. Wegwitz F, Prokakis E, Pejkovska A, Kosinsky RL, Glatzel M, Pantel K, Wikman H, Johnsen SA. 2020. The histone H2B ubiquitin ligase RNF40 is required for HER2-driven mammary tumorigenesis. Cell Death Dis 11:873. https://doi.org/10.1038/s41419-020-03081-w.
12. Dickson K-A, Cole AJ, Gill AJ, Clarkson A, Gard GB, Chou A, Kennedy CJ, Henderson BR, Australian Ovarian Cancer Study (AOCS), Fereday S, Traficante N, Alsop K, Bowtell DD, deFazio A, Clifton-Bligh R, Marsh DJ. 2016. The RING finger domain E3 ubiquitin ligases BRCA1 and the RNF20/RNF40 complex in global loss of the chromatin mark histone H2B monoubiquitination (H2Bub1) in cell line models and primary high-grade serous ovarian cancer. Hum Mol Genet 25:5460–5471. https://doi.org/10.1093/hmg/ddw362.
13. Marsh DJ, Ma Y, Dickson KA. 2020. Histone monoubiquitination in chromatin remodelling: focus on the histone H2B interactome and cancer. Cancers (Basel) 12:3462. https://doi.org/10.3390/cancers12113462.
14. Vousden KH, Prives C. 2009. Blinded by the light: the growing complexity of p53. Cell 137:413–431. https://doi.org/10.1016/j.cell.2009.04.037.
15. Kussie PH, Gorina S, Marechal V, Elenbaas B, Moreau J, Levine AJ, Pavletich NP. 1996. Structure of the MDM2 oncoprotein bound to the p53 tumor suppressor transactivation domain. Science 274:948–953. https://doi.org/10.1126/science.274.5289.948.
16. Kruse JP, Gu W. 2009. Modes of p53 regulation. Cell 137:609–622. https://doi.org/10.1016/j.cell.2009.04.050.
17. Kulikov R, Letienne J, Kaur M, Grossman SR, Arts J, Blattner C. 2010. Mdm2 facilitates the association of p53 with the proteasome. Proc Natl Acad Sci U S A 107:10038–10043. https://doi.org/10.1073/pnas.0911716107.
18. Haupt Y, Maya R, Kazaz A, Oren M. 1997. Mdm2 promotes the rapid degradation of p53. Nature 387:296–299. https://doi.org/10.1038/387296a0.
19. Wade M, Li YC, Wahl GM. 2013. MDM2, MDMX and p53 in oncogenesis and cancer therapy. Nat Rev Cancer 13:83–96. https://doi.org/10.1038/nrc3430.
20. Karni-Schmidt O, Lokshin M, Prives C. 2016. The roles of MDM2 and MDMX in cancer. Annu Rev Pathol 11:617–644. https://doi.org/10.1146/annurev-pathol-012414-040349.
21. Zhao K, Yang Y, Zhang G, Wang C, Wang D, Wu M, Mei Y. 2018. Regulation of the Mdm2-p53 pathway by the ubiquitin E3 ligase MARCH7. EMBO Rep 19:305–319. https://doi.org/10.15252/embr.201744465.
22. Nijman SMB, Lun-Vargas MPA, Velds A, Brummelkamp TR, Dirac AMG, Sixma TK, Bernards R. 2005. A genomic and functional inventory of deubiquitinating enzymes. Cell 123:773–786. https://doi.org/10.1016/j.cell.2005.11.007.
23. Nicassio F, Corrado N, Vissers JHA, Areces LB, Bergink S, Marteijn JA, Geverts B, Houtsmuller AB, Vermeulen W, Di Fiore PP, Citterio E. 2007. Human USP3 is a chromatin modifier required for S phase progression and genome stability. Curr Biol 17:1972–1977. https://doi.org/10.1016/j.cub.2007.10.034.
24. Knaap JA, Kumar BRP, Moshkin YM, Langenberg K, Krijgsveld J, Heck AJR, Karch F, Verrijzer C. 2005. GMP synthetase stimulates histone H2B deubiquitylation by the epigenetic silencer USP7. Mol Cell 17:695–707. https://doi.org/10.1016/j.molcel.2005.02.013.
25. Long L, Thelen JP, Furgason M, Haj-Yahya M, Brik A, Cheng D, Peng J, Yao T. 2014. The U4/U6 recycling factor SART3 has histone chaperone activity and associates with USP15 to regulate H2B deubiquitination. J Biol Chem 289:8916–8930. https://doi.org/10.1074/jbc.M114.551754.
26. Zhang XY, Varthi M, Sykes SM, Phillips C, Warzecha C, Zhu W, Wyce A, Thorne AW, Berger SL, McMahon SB. 2008. The putative cancer stem cell marker USP22 is a subunit of the human SAGA complex required for activated transcription and cell-cycle progression. Mol Cell 29:102–111. https://doi.org/10.1016/j.molcel.2007.12.015.
27. Fuchs G, Shema E, Vesterman R, Kotler E, Wolchinsky Z, Wilder S, Golomb L, Pribluda A, Zhang F, Haj-Yahya M, Feldmesser E, Brik A, Yu X, Hanna J, Aberdam D, Domany E, Oren M. 2012. RNF20 and USP44 regulate stem cell differentiation by modulating H2B monoubiquitylation. Mol Cell 46:662–673. https://doi.org/10.1016/j.molcel.2012.05.023.
28. Zhang Z, Jones A, Joo H-Y, Zhou D, Cao Y, Chen S, Erdjument-Bromage H, Renfrow M, He H, Tempst P, Townes TM, Giles KE, Ma L, Wang H. 2013. USP49 deubiquitinates histone H2B and regulates cotranscriptional pre-mRNA splicing. Genes Dev 27:1581–1595. https://doi.org/10.1101/gad.211037.112.
29. Li M, Chen D, Shiloh A, Luo J, Nikolaev AY, Qin J, Gu W. 2002. Deubiquitination of p53 by HAUSP is an important pathway for p53 stabilization. Nature 416:648–653. https://doi.org/10.1038/nature737.
30. Song MS, Salmena L, Carracedo A, Egia A, Lo-Coco F, Teruya-Feldstein J, Pandolfi PP. 2008. The deubiquitinylation and localization of PTEN are regulated by a HAUSP-PML network. Nature 455:813–817. https://doi.org/10.1038/nature07290.
31. Horst A, Vries-Smits AMM, Brenkman AB, Triest MH, Broek NH, Colland F, Maurice MM, Burgering BMT. 2006. FOXO4 transcriptional activity is regulated by monoubiquitination and USP7/HAUSP. Nat Cell Biol 8:1064–1073. https://doi.org/10.1038/ncb1469.
32. Nicholson B, Kumar K. 2011. The multifaceted roles of USP7: new therapeutic opportunities. Cell Biochem Biophys 60:61–68. https://doi.org/10.1007/s12013-011-9185-5.
33. Li M, Brooks CL, Ning K, Gu W. 2004. A dynamic role of HAUSP in the p53-Mdm2 pathway. Mol Cell 13:879–886. https://doi.org/10.1016/S1097-2765(04)00157-1.
34. Cummins JM, Rago C, Kohli M, Kinzler KW, Lengauer C, Vogelstein B. 2004. Tumour suppression: disruption of HAUSP gene stabilizes p53. Nature 428:1–2. https://doi.org/10.1038/nature02501.
35. Luo K, Li Y, Yin Y, Li L, Wu C, Chen Y, Nowsheen S, Hu Q, Zhang L, Lou Z, Yuan J. 2017. USP49 negatively regulates tumorigenesis and chemoresistance through FKBP51-AKT signaling. EMBO J 36:1434–1446. https://doi.org/10.15252/embj.201695669.
36. Tu R, Kang W, Yang X, Zhang Q, Xie X, Liu W, Zhang J, Zhang XD, Wang H, Du RL. 2018. USP49 participates in the DNA damage response by forming a positive feedback loop with p53. Cell Death Dis 9:553. https://doi.org/10.1038/s41419-018-0475-3.
37. Shalem O, Sanjana NE, Hartenian E, Shi X, Scott DA, Mikkelson T, Heckl D, Ebert BL, Root DE, Doench JG, Zhang F. 2014. Genome-scale CRISPR-Cas9 knockout screening in human cells. Science 343:84–87. https://doi.org/10.1126/science.1247005.
38. Cole AJ, Dickson KA, Liddle C, Stirzaker C, Shah JS, Clifton-Bligh R, Marsh DJ. 2021. Ubiquitin chromatin remodelling after DNA damage is associated with the expression of key cancer genes and pathways. Cell Mol Life Sci 78:1011–1027. https://doi.org/10.1007/s00018-020-03552-5.
39. Kwasna D, Abdul Rehman SA, Natarajan J, Matthews S, Madden R, De Cesare V, Weidlich S, Virdee S, Ahel I, Gibbs-Seymour I, Kulathu Y. 2018. Discovery and characterization of ZUFSP/ZUP1, a distinct deubiquitinase class important for genome stability. Mol Cell 70:150–164. https://doi.org/10.1016/j.molcel.2018.02.023.
40. Xu X, Li S, Cui X, Han K, Wang J, Hou X, Cui L, He S, Xiao J, Yang Y. 2019. Inhibition of ubiquitin specific protease 1 sensitizes colorectal cancer cells to DNA-damaging chemotherapeutics. Front Oncol 9:1406. https://doi.org/10.3389/fonc.2019.01406.
41. Yun S, Kim HH, Yoon JH, Park WS, Hahn MJ, Kim HC, Chung CH, Kim KK. 2015. Ubiquitin specific protease 4 positively regulates the WNT/β-catenin signaling in colorectal cancer. Mol Oncol 9:1834–1851. https://doi.org/10.1016/j.molonc.2015.06.006.
42. Xing C, Lu X-X, Guo P-D, Shen T, Zhang S, He X-S, Gan W-J, Li X-M, Wang J-R, Zhao Y-Y, Wu H, Li J-M. 2016. Ubiquitin-specific protease 4-mediated deubiquitination and stabilization of PRL-3 is required for potentiating colorectal oncogenesis. Cancer Res 76:83–95. https://doi.org/10.1158/0008-5472.CAN-14-3595.
43. Xu X, Huang A, Cui X, Han K, Hou X, Wang Q, Cui L, Yang Y. 2019. Ubiquitin specific peptidase 5 regulates colorectal cancer cell growth by stabilizing Tu translation elongation factor. Theranostics 9:4208–4220. https://doi.org/10.7150/thno.33803.
44. Wu C, Luo K, Zhao F, Yin P, Song Y, Deng M, Huang J, Chen Y, Li L, Lee S, Kim J, Zhou Q, Tu X, Nowsheen S, Luo Q, Gao X, Lou Z, Liu Z, Yuan J. 2018. USP20 positively regulates tumorigenesis and chemoresistance through

β-catenin stabilization. Cell Death Differ 25:1855–1869. https://doi.org/10.1038/s41418-018-0138-z.
45. Diefenbacher ME, Popov N, Blake SM, Schülein-Völk C, Nye E, Spencer-Dene B, Jaenicke LA, Eilers M, Behrens A. 2014. The deubiquitinase USP28 controls intestinal homeostasis and promotes colorectal cancer. J Clin Invest 124:3407–3418. https://doi.org/10.1172/JCI73733.
46. Zhang S, Ju X, Yang Q, Zhu Y, Fan D, Su G, Kong L, Li Y. 2021. USP47 maintains the stemness of colorectal cancer cells and is inhibited by parthenolide. Biochem Biophys Res Commun 562:21–28. https://doi.org/10.1016/j.bbrc.2021.05.017.
47. Zhong J, Zhao M, Ma Y, Luo Q, Liu J, Wang J, Yuan X, Sang J, Huang C. 2012. UCHL1 acts as a colorectal cancer oncogene via activation of the beta-catenin/TCF pathway through its deubiquitinating activity. Int J Mol Med 30:430–436. https://doi.org/10.3892/ijmm.2012.1012.
48. Kosinsky RL, Zerche M, Saul D, Wang X, Wohn L, Wegwitz F, Begus-Nahrmann Y, Johnsen SA. 2020. USP22 exerts tumor-suppressive functions in colorectal cancer by decreasing mTOR activity. Cell Death Differ 27:1328–1340. https://doi.org/10.1038/s41418-019-0420-8.
49. Li X, Stevens PD, Yang H, Gulhati P, Wang W, Evers BM, Gao T. 2013. The deubiquitination enzyme USP46 functions as a tumor suppressor by controlling PHLPP-dependent attenuation of Akt signaling in colon cancer. Oncogene 32:471–478. https://doi.org/10.1038/onc.2012.66.
50. Jansson MD, Damas ND, Lees M, Jacobsen A, Lund AH. 2015. miR-339-5p regulates the p53 tumor-suppressor pathway by targeting *MDM2*. Oncogene 34:1908–1918. https://doi.org/10.1038/onc.2014.130.
51. Zhang C, Liu J, Tan C, Yue X, Zhao Y, Peng J, Wang X, Laddha SV, Chan CS, Zheng S, Hu W, Feng Z. 2016. MicroRNA-1827 represses *MDM2* to positively regulate tumor suppressor p53 and suppress tumorigenesis. Oncotarget 7:8783–8796. https://doi.org/10.18632/oncotarget.7088.
52. Seligson ND, Stets CW, Demoret BW, Awasthi A, Grosenbacher N, Shakya R, Hays JL, Chen JL. 2019. Inhibition of histone deacetylase 2 reduces MDM2 expression and reduces tumor growth in dedifferentiated liposarcoma. Oncotarget 10:5671–5679. https://doi.org/10.18632/oncotarget.27144.
53. Liu X, Tan Y, Zhang C, Zhang Y, Zhang L, Ren P, Deng H, Luo J, Ke Y, Du X. 2016. NAT10 regulates p53 activation through acetylating p53 at K120 and ubiquitinating Mdm2. EMBO Rep 17:349–366. https://doi.org/10.15252/embr.201540505.
54. Shechter D, Dormann HL, Allis CD, Hake SB. 2007. Extraction, purification and analysis of histones. Nat Protoc 2:1445–1457. https://doi.org/10.1038/nprot.2007.202.